



HAL
open science

Clustering and internalization of integrin alphavbeta3 with a tetrameric RGD-synthetic peptide.

Lucie Sancey, Elisabeth Garanger, Stéphanie Foillard, Guy Schoehn,
Amandine Hurbin, Corinne Albiges-Rizo, Didier Boturyn, Catherine Souchier,
Alexei Grichine, Pascal Dumy, et al.

► To cite this version:

Lucie Sancey, Elisabeth Garanger, Stéphanie Foillard, Guy Schoehn, Amandine Hurbin, et al.. Clustering and internalization of integrin alphavbeta3 with a tetrameric RGD-synthetic peptide.. *Molecular Therapy*, 2009, 17 (5), pp.837-43. 10.1038/mt.2009.29 . inserm-00369024

HAL Id: inserm-00369024

<https://www.hal.inserm.fr/inserm-00369024>

Submitted on 7 Sep 2009

HAL is a multi-disciplinary open access archive for the deposit and dissemination of scientific research documents, whether they are published or not. The documents may come from teaching and research institutions in France or abroad, or from public or private research centers.

L'archive ouverte pluridisciplinaire **HAL**, est destinée au dépôt et à la diffusion de documents scientifiques de niveau recherche, publiés ou non, émanant des établissements d'enseignement et de recherche français ou étrangers, des laboratoires publics ou privés.

Clustering and internalization of integrin $\alpha_v\beta_3$ with a tetrameric RGD-synthetic peptide

Sancey Lucie¹⁻², Garanger Elisabeth¹⁻²⁻³, Foillard Stéphanie²⁻³, Schoehn Guy⁴⁻⁵, Hurbin Amandine¹⁻², Albiges-Rizo Corinne²⁻⁶⁻⁷, Boturyn Didier²⁻³, Souchier Catherine²⁻⁸, Grichine Alexei²⁻⁸, Dumy Pascal²⁻³, Coll Jean-Luc¹⁻²

¹ INSERM CRI U823, Cibles diagnostiques ou thérapeutiques et vectorisation de drogues dans les cellules tumorales, Institut Albert Bonniot, BP 170, 38 042 Grenoble cedex 9, France

² Université Joseph Fourier, BP 53, 38 041 Grenoble cedex 9, France

³ Département de Chimie Moléculaire, CNRS, UMR-5250, BP 53, 38 041 Grenoble cedex 9, France

⁴ Université Joseph Fourier, Unit for Virus Host Cell Interaction, UMR 5233 UJF-EMBL-CNRS, BP 181, 38042 Grenoble cedex 9, France

⁵ Institut de Biologie Structurale Jean-Pierre Ebel, UMR5075 CEA-CNRS-UJF, 41 rue Jules Horowitz, 38027 Grenoble cedex 1, France

⁶ INSERM CRI U823, Dynamique des systèmes d'adhérence, différenciation cellulaire et oncogenèse, Institut Albert Bonniot BP 170, 38 042 Grenoble cedex 9, France

⁷ ERL CNRS 3148, Institut Albert Bonniot BP 170, 38 042 Grenoble cedex 9, France

⁸ INSERM CRI U823, Stress et dynamique de l'organisation du génome, Institut Albert Bonniot BP 170, 38 042 Grenoble cedex 9, France

Running title: Tetrameric RGD vector targeting integrin $\alpha_v\beta_3$

Correspondance should be adressed to: Dr Coll Jean-Luc, INSERM U823, Equipe 5, Institut Albert Bonniot, BP 170, 38 042 Grenoble cedex 9, France.

Phone: 33 [0]4 76 54 95 53 / Fax: 33 [0]4 76 54 94 13

E-mail: Jean-Luc.Coll@ujf-grenoble.fr

Integrin $\alpha_v\beta_3$ is overexpressed on neoendothelial cells and frequently on tumor cells. We have developed a peptide-like scaffold (RAFT), which holds 4 *cyclo*[-RGDfK-] (cRGD) motifs and proved that this molecule (called RAFT-RGD) targets integrin $\alpha_v\beta_3$ *in vitro* and *in vivo*. Using Fluorescence Correlation Spectroscopy, we measured the constant of affinity (K_D) of the RAFT-RGD for purified integrins. K_D values rose from 3.87 nM for RAFT-RGD to 41.70 nM for *cyclo*[-RGDfK-]. In addition RAFT-RGD inhibited $\alpha_v\beta_3$ lateral mobility in the cell membrane, due to the formation of integrin-clusters as demonstrated by Fluorescence Recovery after Photobleaching. This was confirmed by electronic microscopy data, which established the formation of molecular complexes containing 2 integrins in the presence of RAFT-RGD but not cRGD or RAFT-RAD. Using an Enzyme-Linked ImmunoSorbent Assay, we proved that 1 μ M RAFT-RGD increased by 79% $\alpha_v\beta_3$ internalization via clathrin-coated vesicles. Conversely, cRGD was internalized without modifying $\alpha_v\beta_3$ internalization. Although RGD has been known for more than 20 years, this is the first study to formerly establish the relationships between multimeric presentation, increased affinity and subsequent integrin mediated co-internalization. These results strongly support the rationale for using multimeric RGD peptides as targeting vectors for imaging, diagnosis or therapy of cancers.

Key words: integrin internalization, RGD-peptide, angiogenesis, cancer, carrier

Introduction

Targeting tumor angiogenesis for specific drug transfer into tumor masses and metastasis has been identified as a promising approach for three main reasons: i) angiogenesis is a common and genetically stable characteristic of most solid tumors, ii) it is readily accessible from the blood stream and iii) it can be targeted by specific RGD-containing peptides binding integrin $\alpha_v\beta_3$. This integrin is indeed poorly expressed on quiescent vessels and is selectively overexpressed on activated endothelial cells of growing vessels. In addition, integrin $\alpha_v\beta_3$ is also frequently overexpressed on tumor cells, as observed in lung cancers [1, 2], melanomas [3], brain tumors [4] or breast cancers [5].

Integrins are membrane-spanning heterodimers of α and β subunits, both of which comprise a short cytoplasmic tail, a single transmembrane helix and a large extracellular domain [6]. Most integrins are expressed in a default low-affinity ligand-binding state but their conformation and affinity can vary in response to cellular and microenvironment stimulations [7, 8]. This will also affect their lateral assembly and clustering on the surface of the cell [9]. Several groups have developed multimeric RGD-presenting molecules, with the aim not only to increase integrin affinity and clustering but also to induce an active integrin-mediated internalization [10-12].

We have developed a Regioselectively Addressable Functionalized Template (RAFT) cyclo-decapeptide scaffold, able to present 4 cyclic RGD pentapeptide motifs. We have shown using nuclear or optical imaging methods, that RAFT-RGD allows an improved and $\alpha_v\beta_3$ -specific targeting and drug delivery [13] as well as *in vivo* imaging of tumors as compared to the monomeric cyclic RGD (cRGD) [14-17].

Surprisingly, while the interaction between RGD-ligands and integrins has been known for a long time [18, 19] and RGD-containing molecules been widely used to deliver various kinds of

cargos including nanoparticles (liposomes or polymers), cytotoxic peptides, low molecular weight drugs and contrast-enhancing agents (fluorochromes, radiotracers) [12, 20-22], very little is known about the internalization mechanism of RGD peptides binding to integrin $\alpha_v\beta_3$.

Two studies have described how an antibody directed against integrin $\alpha_v\beta_3$ (mAb 17E6) and monomeric or multimeric RGD peptides are internalized. Both concluded that the internalization of monomeric RGD ligands is independent of its $\alpha_v\beta_3$ receptor and occurs via a fluid-phase endocytic pathway. In contrast, multimeric RGD molecules are co-internalized with their receptor [23, 24], evidence in favor of integrin aggregation and clustering.

The integrin endo/exocytic cycle [25-27] suggests that there are, at least, three types of pathways associated with integrin internalization: 1/ clathrin-mediated endocytosis was described for $\alpha_v\beta_5$ integrins [28]; 2/ caveolae-mediated endocytosis for α_2 integrins [29] and 3/ clathrin-caveolae-independent endocytosis. To our knowledge, endocytosis of $\alpha_v\beta_3$ integrins was described to occur through clathrin-dependent endocytosis [30] or uncoated vesicles [31]. Clathrin-dependent endocytosis has also been described for viruses such as adenoviruses that enter the cells after binding to the $\alpha_v\beta_3$ integrin secondary receptor [32].

Here, we studied the biological properties of the tetrameric RAFT-RGD peptide (coupled or not to fluorescent probes) as compared to those of its monomeric counterpart cRGD so as to better understand and improve the potential of RGD-based vectors to specifically deliver therapeutic drugs directly inside the target cells. We measured their affinity (K_D) for the purified integrin $\alpha_v\beta_3$ in solution.

Results

Affinities of RAFT-RGD versus cRGD for the purified, soluble integrin $\alpha_v\beta_3$.

Fluorescence correlation spectroscopy (FCS) is commonly used to characterize the dynamics of fluorescent molecules in solution. This technique allows users to measure fluorescence intensity fluctuations due to diffusion phenomenon, chemical reactions, aggregation... We first established the diffusion properties of each fluorescently labeled RGD-containing molecules in solution and then measured the variation of this parameter in the presence of a large excess of purified integrins. This provided quantitative information allowing the determination of a constant of association (K_D).

FCS analysis indicated that the tetrameric RAFT-RGD-Cy5 had a 10-fold higher affinity for its soluble receptor integrin $\alpha_v\beta_3$ in HBSS (containing Ca^{2+}/Mg^{2+}) than the monomeric cRGD-Cy5 (Fig. 1b). Its dissociation constant (K_D), obtained by curve fitting with a two-component model, was 3.87 nM while the K_D of cRGD-Cy5 reached 41.70 nM. The non-specific RAFT-RAD-Cy5 did not interact with integrin $\alpha_v\beta_3$: the data fitted neither a two- nor even a three-component model but only fitted a one-component model, corresponding to free RAFT-RAD-Cy5. The K_D of RAFT-RGD-Cy5 was also determined for a non-specific receptor integrin $\alpha_3\beta_1$: in this case, the measured K_D was 1147 nM, *i.e.* 300 fold higher than the one obtained with $\alpha_v\beta_3$.

RAFT-RGD slows down integrin $\alpha_v\beta_3$ mobility in the cell membrane

We measured the mobility of integrin $\alpha_v\beta_3$ in the membrane of adherent HEK293(β_3) cells in the presence of the different peptides by FRAP analysis using a confocal microscope. These cells expressing natural amount of the human α_v chain were stably transfected with a plasmid encoding for the human β_3 chain. We focused the laser beam on the apical membrane for two

reasons: 1/ integrins from this region are mobile because they are not engaged in cell-matrix adhesions and 2/ this area is less affected by cell shrinkage usually observed in the presence of RGD peptides. Adherent cells were co-incubated for 8 min with the different peptides and the R-PhycoErythrin-labeled LM609 antibody. After the RPE photobleaching in a defined area (ROI), the time for fluorescence recovery due to the lateral movement of RPE-labeled integrins on the membrane was measured (Fig. 2). Importantly, we initially verified that LM609's binding was not affected by the presence of the peptides (data not shown). Also, no significant cellular movement or changes in membrane curvature occurred during fluorescence sampling. Results presented in Fig. 2 indicate that the presence of RAFT-RGD-FITC peptide dramatically slowed down the recovery of the integrin signal into the bleached area as compared to untreated cells. In contrast, no decrease in the time of recovery was observed either by using the negative control peptide RAFT-RAD-FITC or with the monovalent cRGD-FITC. The apparent diffusion time, calculated from the fluorescence recovery curves obtained on twenty individual cells (three separated experiments), increased from 46 ± 14 seconds (RAFT-RAD-FITC, cRGD-FITC and PBS) to 144 ± 22 seconds (RAFT-RGD-FITC). No concomitant change in peptide distribution was induced during FRAP experiments as monitored in the FITC detection channel. The fluorescence recovery being directly correlated to the mobility of the receptor, these results suggested that the presence of the tetrameric RAFT-RGD-FITC slowed down $\alpha_v\beta_3$ integrin diffusion within the cell membrane by linking several integrins together, *i.e.* by clustering integrins.

RAFT-RGD can bind two $\alpha_v\beta_3$ integrins simultaneously

In order to confirm the data obtained by FRAP, we aimed at visualizing the possible formation of integrin clusters induced by RAFT-RGD. We used negative staining electron microscopy to observe $\alpha_v\beta_3$ integrin and $\alpha_v\beta_3$ /RGD-peptides mixed in 1 mM Mg^{2+}/Ca^{2+} as illustrated in Fig. 3. Peptides were used in excess as compared to the integrin concentration. These conditions are not supposed to maximize the number of dimers. Integrins alone or mixed with cRGD or RAFT-RAD displayed compact particles representing single heterodimers of $\alpha_v\beta_3 \pm$ RGD as expected. Indeed, the monomeric cRGD does not have the possibility to interact with several integrins at the same time, while the RAFT-RAD is not able to recognize them at all. Conversely $\alpha_v\beta_3$ /RAFT-RGD micrographs were frequently showing larger particles corresponding to complexes of two $\alpha_v\beta_3$ integrins probably linked by the multimeric RAFT-RGD. Visually, we estimated that about 10% of $\alpha_v\beta_3$ /RAFT-RGD were forming integrin dimers. But, this percentage was most probably underestimated because we counted only the aggregates laying on the grid in a proper angle of examination and providing particles with this typical dimer-shape. For example, clusters viewed down the long axis would appear more compact [33] and were not included (the staining agent outlines only those parts of the objects that are in contact with the carbon film). Nevertheless, electron microscopy is a qualitative technique and not a quantitative technique: dimers of integrins may bind with less affinity to the carbon than monomeric integrins, thus leading to underestimate the number of dimers.

RAFT-RGD-mediated integrin $\alpha_v\beta_3$ internalization

RAFT-RGD-Cy5 and cRGD-Cy5 internalizations were observed by confocal microscopy on live HEK293(β_3) cells (Fig. 4). RAFT-RGD-Cy5 was rapidly internalized in small vesicles after 10 min (Fig. 4a) but was also found in the cytoplasm and at cell-cell contacts. Monomeric cRGD-

Cy5 internalization is less extensive than that of RAFT-RGD-Cy5 and the laser intensity had to be increased three times in order to obtain comparable signal intensities (Fig. 4E).

We then developed a special ELISA assay to demonstrate that RGD-peptides were inducing integrin $\alpha_v\beta_3$ internalization. Briefly, integrins exposed on the surface of HEK293(β_3) cells were biotinylated and the cells were incubated in the presence of 0 to 1 μM RAFT-RGD or 0 to 4 μM cRGD for 10 min in order to keep the number of RGD motifs constant. The cells were then lysed, fractionated and the concentration of biotinylated- $\alpha_v\beta_3$ -integrins present into each fraction measured using ELISA. The absence of peptide (control condition) established the normal endocytosis of integrin $\alpha_v\beta_3$; we found that $12 \pm 1\%$ of the labeled integrins are internalized “naturally” in 10 min (Table 1). In the presence of RAFT-RGD, internalization increased in a dose-dependent manner and reached $21 \pm 2\%$ at 1 μM , corresponding to an increase of 79% vs. control. In contrast, increasing doses of cRGD (from 0.1 to 4 μM) did not affect integrin internalization at all, which remained similar to that of the control (*i.e.* $12 \pm 1\%$ at 1 μM).

Altogether this indicated that RAFT-RGD internalization was correlated with integrin $\alpha_v\beta_3$ endocytosis, while the monomeric cRGD did not affect $\alpha_v\beta_3$ natural endocytosis.

RAFT-RGD internalization occurs via clathrin-mediated endocytosis

RAFT-RGD-Cy5 and cRGD-Cy5 internalization pathways were analyzed using confocal microscopy in the presence of specific inhibitors (Fig. 4). In the presence of the clathrin-inhibitor amantadine at 1 mM (Fig. 4b), RAFT-RGD-Cy5 internalization was extensively inhibited. The fluorescence was found at the cell surface mainly and especially at the cell-cell contacts. In contrast, amantadine did not affect cRGD-Cy5 internalization (compare Fig. 4e and 4f). One μM of nystatin, an inhibitor of caveolae-dependent internalization had no effect on either peptide

(Fig. 4c and 4g). In the presence of 1 mM amiloride, internalization of the peptides remained unchanged (Fig. 4d and 4h) although, we proved by using 70 kDa-dextran-FITC, that macropinocytose was correctly inhibited in these cells (data not shown).

These results were confirmed by the ELISA measurements of the integrin $\alpha_v\beta_3$ amount internalized after binding to RAFT-RGD in the presence of amantadine, nystatin or amiloride (Table 1). In the presence of amantadine, 1 μ M of RAFT-RGD was not able any more to induce integrin internalization and the % of internalized integrins was exactly similar to the control values ($12 \pm 2\%$). In contrast, nystatin or amiloride did not prevent RAFT-RGD-induced integrin $\alpha_v\beta_3$ internalization. These data suggested that RAFT-RGD was internalized with integrin $\alpha_v\beta_3$ via the clathrin-dependent pathway. Furthermore, peptides internalization was quantified from confocal microscopy analysis. The related peptide internalization indexes are reported Figure 4 (mean of Cy5-intensity/pixels). Those indexes confirmed that RAFT-RGD internalization occurred in a clathrin-dependent pathway, but also that RAFT-RGD gets into the cells more efficiently than cRGD.

Discussion

Drug vectorization mediated by specific tumor-targeting molecules could allow specific delivery of cytotoxic agents to tumors therefore limiting their systemic toxicity. Based on this concept, RGD-containing peptides have been largely used for the targeting of $\alpha_v\beta_3$ -integrin expressing tumors and/or of their microvasculature. Our group contributed to the development of a synthetic multimeric RGD-based vector, called RAFT-RGD. This peptide proved to be particularly

efficient for the delivery of drugs, imaging agents or both [14-16, 17, 34]. However, although RGD-integrin interaction has been discovered a long time ago [18, 19], the mechanism of internalization of monomeric or multimeric RGD peptides is a poorly documented process. In this study, we focused our attention to the study of the mechanism by which the well-known cRGD, similar to the original cyclic peptide developed by Kessler et al. [35, 36] and its RAFT-supported tetrameric version RAFT-RGD are internalized, with a particular emphasis on the internalization pathways involved after recognition and binding to the $\alpha_v\beta_3$ receptor.

Multimeric RGD-peptides are expected to present an increased affinity for the $\alpha_v\beta_3$ integrin as compared to their monomeric counterpart. This has been demonstrated when comparing cyclic versus linear RGD-based peptides [37, 38]. We confirmed this characteristic for the RAFT-RGD using an FCS assay. RAFT-RGD-Cy5 bound specifically to integrin $\alpha_v\beta_3$ with a 10 fold higher affinity than cRGD (Fig. 1b). Surprisingly, although integrins are known to present at least two affinity states, we measured only one K_D value for both RAFT-RGD-Cy5 and cRGD-Cy5. In addition, the K_D value measured for cRGD was about 25 times higher than previously reported values [38, 39]. This suggested that, in our FCS assay, integrins were exclusively in their activated form as a result of the combined presence of octyl- β -D-glucopyranoside (unpublished observations), Mg^{2+} ions [40, 41] and of cRGD peptides [9, 42] in the media, each of these factors being known to switch integrins in their high affinity state. In addition, it must be noticed that previous measurements of the K_D described in the literature were based on solid-phase receptor binding assays. In our case, integrins were in solution and this certainly modified their constant of affinity.

Using FRAP, we also demonstrated that the multimeric RAFT-RGD decreased the lateral mobility of $\alpha_v\beta_3$ receptors on the surface of HEK293(β_3) cells. This suggested that the presence

of four cRGD motifs onto the RAFT scaffold allowed the clustering of integrin $\alpha_v\beta_3$. This result is important because it suggested at least two cRGD motifs presented by a single RAFT molecule can bind two integrins. This was an open challenge for the RAFT scaffold, which is no more than 10 Å large. Indeed, the three-dimensional structure of purified $\alpha_v\beta_3$ integrin showed that the diameter of this integrin is close to 100 Å [39], but that the RGD binding site is on the periphery of the molecule. The 2 RGD motifs presented by a single RAFT could thus bridge 2 integrins positioned back to back. This was confirmed by EM results, which indicated that the tetrameric, but not the monomeric cRGD, could form clusters of 2 integrins. Formation of these $\alpha_v\beta_3$ clusters was then immediately followed by an active internalization of the tetrameric RAFT-RGD-Cy5 via, and concomitantly with integrin $\alpha_v\beta_3$. Indeed, the natural endocytosis of this integrin almost doubled in less than 10 min in the presence of RAFT-RGD and its internalization was mainly involving clathrin-mediated endocytosis. Accordingly, this process was abolished in the presence of amantadine, a specific inhibitor of the clathrin-mediated endocytosis. Macropinocytosis and caveolae-mediated endocytosis may not be implicated since their inhibitors like amiloride or nystatin had no effect on RAFT-RGD internalization. Interestingly, the monomeric cRGD peptide interacted in a completely different manner. Its internalization did not rely on clathrin- or caveolae-mediated endocytosis and was most probably independent of $\alpha_v\beta_3$ because of the internalization of the integrin which was not affected. These results are in agreement with a previous report and indicated that cRGD can probably cross cell membranes via a fluid-phase pathway [24]. The corresponding efficiency of internalization is however much less efficient than that of the RAFT-RGD, which explains the lower intensity of staining of the inside of cells labeled with cRGD-Cy5 and as demonstrated by the indexes in Figure 4.

Viruses such as foot-and-mouth disease virus [43] or adenovirus present several RGD motifs allowing their interaction with the $\alpha_v\beta_3$ integrin. This interaction is a prerequisite to their internalization [32, 44], which also occurs via clathrin-coated vesicles [45]. RAFT-RGD may thus mimic some properties of these viruses.

In summary, the tetrameric RAFT-RGD binds 10 times more strongly to its $\alpha_v\beta_3$ receptor than cRGD. RAFT-RGD is actively and efficiently internalized with integrin $\alpha_v\beta_3$ via clathrin-coated pits as previously described for the $\alpha_v\beta_3$ integrin [46]. This contrasts with the trafficking route followed by the β_1 integrin, which was shown to use preferentially a caveolae-dependent pathway [47]. Efficient internalization is of course an important issue for drug delivery and we proved that this RAFT-RGD molecule is indeed capable of inducing a specific and efficient targeted intracellular delivery of a toxic peptide able to destabilize mitochondria [13].

From this study, multimeric presentation of cRGD motifs appears to be a prerequisite for the development of efficient integrin targeting and cell internalizing vectors for drug delivery to tumors.

Materials and Methods

Material

Integrin $\alpha_v\beta_3$ was purchased from Chemicon International (CC1021, St Quentin en Yvelines, France). Monoclonal antibody anti-human integrin $\alpha_v\beta_3$ LM609 conjugated to R-PhycoErythrin (RPE-LM609) and anti-human CD61 were purchased from Chemicon and Beckman Coulter

respectively (IM0540, Villepinte, France). Cycloheximide was from Sigma Aldrich (Lyon, France). NHS-SS-biotin was from Pierce (21441, Brebières, France).

RGD-Peptides Synthesis and Fluorescent Labeling

Compounds were synthesized according to previously reported procedures [34] and chemical structures are presented in Fig. 1a. Briefly, RAFT is a cyclic decapeptide (c [-Lys(Boc)-Lys(Alloc)-Lys(Boc)-Pro-Gly-Lys(Boc)-Lys(Alloc)-Lys(Boc)-Pro-Gly-]) having two orthogonally addressable domains pointing on either side of the cyclopeptide backbone. On the upper face, four copies of the c[-RGDfK-] peptide were grafted via an oxime bond (R1-O-N = C-R2) for recognition of the integrin $\alpha_v\beta_3$. On the other side of the RAFT, either Cy5 mono NHS (N-hydroxysuccinimide) ester (Amersham Biosciences, Uppsala, Sweden) or FITC (Sigma-Aldrich, St Quentin Fallavier, France) was added on the lysine chain (c [-KKKPGKAKPG-]) [17]. As a negative control probe, Cy5-labeled RAFT(c[-R β ADfK-])₄ (RAFT-RAD) was also synthesized in a similar way.

FCS analysis

FCS study was performed on the ConfoCor 2 system (Carl Zeiss, Jena, Germany) using a 40x water immersion C-Apochromat objective lens (numerical aperture (N.A.) = 1.2). The measurements were carried out at room temperature in 8-well Lab-Tek I chambered coverglass (Nalge Nunc Int., Illkirch, France). The 633 nm He-Ne laser beam was focused into 50 μ l solutions at 150 μ m over the cover glass. The fluorescence emission was collected through a pinhole and a 650 nm-long pass filter. Photon counts were detected by an Avalanche PhotoDiode (APD) at 20 MHz for 30 sec. For each sample, FCS measurements were repeated 15 times. The

data evaluation was performed using the Zeiss FCS Fit software. Most of the intensity autocorrelation curves were fitted using a free diffusion model with two components: the peptide coupled to the fluorochrome alone and the fluorescent peptide–integrin complex. Preliminary studies enabled us to determine the diffusion time value of the first component and structural parameter. Moreover, a calibration step with 4 nM Cy5 allowed the evaluation of the size of the confocal volume (≈ 1 fl). Interaction assays were performed at RT in HBSS containing Mg^{2+} and Ca^{2+} . One to 40 nM of soluble integrin $\alpha_v\beta_3$ (CC1021, Chemicon Int., France) were mixed with 0.6 nM of RAFT-RGD-Cy5 and RAFT-RAD-Cy5 or 2.4 nM of cRGD-Cy5. FCS measurements were performed 2 min after mixing. Theoretical calculation was made using the Origin software. The goodness-of-fit (χ^2) was the mean end point for the quality of the fit (in our condition, $5E^{-4} < \chi^2 < 1E^{-6}$ for a good fit). Furthermore, the residual curves had no wavy shape (see example in supplementary data).

Cell Lines and Culture Conditions

HEK293(β_3), stable transfectants of human β_3 from the human embryonic kidney cell line (kindly provided by J-F. Gourvest, Aventis, France), were cultured as described in Jin et al. [15]. The cell line was cultured at 37°C in a humidified 95% air / 5% CO₂ atmosphere.

Confocal Laser Scanning Microscopy and FRAP Experiments

HEK293(β_3) cells were grown for 24 h on 18 mm round cover glasses placed in the wells of a 12-well plate (seeding density of 7×10^4 cells per well). Immediately before running the experiment, cells were incubated for 8 min at RT (22°C) in a mixture of R-PhycoErythrin-conjugated LM609 monoclonal antibody (RPE-LM609, Chemicon Int.) and 0.5 μ M FITC-

labeled RGD peptides. The incubation with monovalent cRGD was performed at either 0.5 μM or 2 μM . The antibody and peptide solutions were extemporaneously prepared in HBS buffer enriched with 1 mM MgCl_2 . For microscopic observations, coverslips were rinsed once in HBS buffer and disposed on a custom-made incubation chamber containing 200 μL of the FITC-labeled RGD peptide solutions (0.5 μM or 2 μM with cRGD). The confocal imaging and FRAP measurements were carried out on an inverted confocal microscope (LSM510, Carl Zeiss, Jena, Germany) using a 40x water immersion objective of 1.2 N.A. A pinhole adjustment resulted in a 2.5 μm optical slice used for the visualization of a 25 μm circular region of the cell apex membrane at scan zoom 4. For FRAP experiments, a 3 μm circular ROI was uniformly bleached for 2 sec with 100% intensity of the 543 nm line (fluorescence bleaching ratio > 90%). The fluorescence recovery was then sampled on the whole region for 170 sec every 5 sec with 0.1% laser intensity set with AOTF. Thanks to the extremely small excitation power and short acquisition times, no photobleaching was induced during sampling as observed on control cells or on the membrane out of the bleached ROI. Neither lateral nor axial displacement of ROI was observed during FRAP measurements and no recovery of fluorescence was observed on the entirely bleached control cells.

Data analysis was performed in assumption that the recovery of fluorescence in the ROI was solely due to the two-dimensional cytoplasmic diffusion of fluorescent species. The diffusion time τd was determined by fitting the normalized fluorescence recovery curves $F(t)$ to the recovery kinetics equation: [48, 49]

$$F(t) = F_0 + [F_\infty - F_0] \cdot \exp\left(\frac{-2\pi d}{t}\right) \cdot \left[I_0\left(\frac{2\pi d}{t}\right) + I_1\left(\frac{2\pi d}{t}\right) \right] \quad (1)$$

where t is time, F_0 and F_∞ are initial and final mean fluorescence intensities after photobleaching respectively, I_0 and I_1 are modified Bessel functions. The diffusion time values obtained for each peptide conditions are the mean of 20 individual cells.

Electron microscopy

Soluble human integrin $\alpha_v\beta_3$ (Chemicon, #CC1021) was diluted to 0.095 mg/ml (≈ 3.65 fmol) in PBS containing $MgCl_2$ and $CaCl_2$ at 1 mM and mixed with RAFT-RGD 0.45 mg/ml (≈ 1 nmol), cRGD 0.1 mg/ml (≈ 1 nmol) or RAFT-RAD 0.45 mg/ml (≈ 1 nmol) for 2 min before addition on top of a carbon-coated electron microscope grid. Thirty sec later, the excess of liquid was removed by blotting with a filter paper. Four ml of a 2 % Uranyl Acetate solution were placed on the grid and incubated for 30 sec - 1 min at room temperature. The staining solution was subsequently removed by filter paper adsorption, and the grid was dried on a paper filter for 2 min and then examined using an electron microscope. Micrographs were taken under low-dose conditions with a Jeol 1200-EX II microscope at 100 kV or a FEI CM12 microscope at 120 kV and a respectively calibrated magnification of 40000 and 45000 times. Selected negatives films were digitalized on a Zeiss scanner (Photoscan TD) with a pixel size of 14 μm , corresponding to 3.5 \AA or 3.1 \AA at the sample scale.

Confocal Microscopy of Peptide Internalization

HEK293(β_3) cells were grown as described in 4-wells Lab-Tek I chambered coverglass. Cells were starved 30 min and incubated with DMEM w/o red phenol alone or containing amantadine 1 mM, nystatin 1 μM or amiloride 1 mM for another 30 min at 37°C, 5% CO_2 . Then, 1 mM RAFT-RGD-Cy5 or 1 mM cRGD-Cy5 were added to the culture medium, together with 5 μM of

Hoechst, for 10 min. Confocal microscopy was performed on the Axiovert 200 LSM510 LNO Meta microscope (Carl Zeiss, Jena, Germany) using a 40x oil immersion objective of 1.2 N.A., after addition of fresh medium. The 633 nm laser intensity was set up on request at 10 or 30% of its maximum intensity depending on the peptide. The following inhibitors were used in order to block caveolae, clathrin-coated pits or macropinocytosis: nystatin 1 μ M, amantadine 1 mM, or amiloride 1 mM (Sigma Aldrich).

Peptides internalization was quantified from confocal microscopy analysis. The mean Cy5 intensity was related to the cell area (in pixel); the related index is reported on the pictures.

Integrin internalization assay

Surface biotin labeling and internalization

HEK293(β_3) cells were cultured at ~85% confluence in 90 mm dishes and starved at 37°C for 30 min in DMEM containing 15 μ M of cycloheximide (Sigma Aldrich, St Quentin Fallavier, France). Membrane labeling was adapted from Roberts et al. [50]. Depending of the condition, cells were kept at 4°C or placed 10 min at 37°C in DMEM alone (control) or containing RAFT-RGD or cRGD from 0.1 to 4 μ M, in order to allow receptor internalization.

In order to measure endocytosis inhibition, amantadine 1 mM, nystatin 1 μ M or amiloride 1mM were added to the medium 30 min before biotin labeling. Those inhibitors were kept in the medium during biotin labeling and peptides internalization.

ELISA

Integrin internalization was quantified using Enzyme Linked ImmunoSorbent Assay in 96-wells plate, through gentle agitation. The previous day, 0.2 μ g of mAb anti-human CD61 (IM0540, Beckman Coulter, France) were used to coat wells (n=3 wells/condition) by incubating overnight

at 4°C under gentle agitation. Antibodies were removed and unspecific sites were blocked with 300 μ l of PBS/BSA 3%/0.05% tween for 1 h at RT. Wells were washed 3 times with 300 μ l PBS/0.05% tween for 5 min before addition of 50 μ g of protein lysates adjusted to 200 μ l with lysis buffer, for 1 h at RT. Wells were washed again 5 times with 300 μ l PBS/0.05% tween for 5 min. Then, 200 μ l of streptavidin-POD/PBS/0.05% tween (1:10000) (11 089 153 001, Roche Diagnostic, Meylan, France) were added on anti-CD61 / biotinylated integrin complex for 1 h at RT. Samples were washed 3 times with 300 μ l PBS/0.05% tween and 2 times with 300 μ l PBS for 5 min. At last, integrin internalization was revealed using ABTS kit (00-2011, Zymed, Cergy Pontoise, France) and quantified as described by the manufacturer. Results were expressed as mean of OD +/- S.E.M. and each experiment was performed in quadruplet at least.

Acknowledgments

This work was supported by the Institut National de la Santé et de la Recherche Médicale (INSERM), the INCA (Institut National for Cancer), the Association for Research on Cancer (ARC, France), the Agence Nationale pour la Recherche (ANR (V2IP and Pepvec programs)) and the EMIL and N2L NoE of the 6th FWP. We also acknowledged Marc Block (ERL CNRS 3148, Institut Albert Bonniot BP 170, 38 042 Grenoble cedex 9, France) for helpful discussion during the redaction of this manuscript.

References

1. Chen, X, Sievers, E, Hou, Y, Park, R, Tohme, M, Bart, R, *et al.* (2005). Integrin alpha v beta 3-targeted imaging of lung cancer. *Neoplasia* **7**: 271-279.
2. Sato, T, Konishi, K, Kimura, H, Maeda, K, Yabushita, K, Tsuji, M, *et al.* (2001). Vascular integrin beta 3 and its relation to pulmonary metastasis of colorectal carcinoma. *Anticancer Res* **21**: 643-647.
3. Seftor, RE, Seftor, EA, Gehlsen, KR, Stetler-Stevenson, WG, Brown, PD, Ruoslahti, E, *et al.* (1992). Role of the alpha v beta 3 integrin in human melanoma cell invasion. *Proc Natl Acad Sci U S A* **89**: 1557-1561.
4. Gladson, CL, and Cheresch, DA (1991). Glioblastoma expression of vitronectin and the alpha v beta 3 integrin. Adhesion mechanism for transformed glial cells. *J Clin Invest* **88**: 1924-1932.
5. Rolli, M, Fransvea, E, Pilch, J, Saven, A, and Felding-Habermann, B (2003). Activated integrin alphavbeta3 cooperates with metalloproteinase MMP-9 in regulating migration of metastatic breast cancer cells. *Proc Natl Acad Sci U S A* **100**: 9482-9487.
6. Hynes, RO (2002). Integrins: bidirectional, allosteric signaling machines. *Cell* **110**: 673-687.
7. Calderwood, DA (2004). Integrin activation. *J Cell Sci* **117**: 657-666.
8. Ginsberg, MH, Partridge, A, and Shattil, SJ (2005). Integrin regulation. *Curr Opin Cell Biol* **17**: 509-516.
9. Cluzel, C, Saltel, F, Lussi, J, Paulhe, F, Imhof, BA, and Wehrle-Haller, B (2005). The mechanisms and dynamics of (alpha)v(beta)3 integrin clustering in living cells. *J Cell Biol* **171**: 383-392.
10. Garanger, E, Boturyn, D, and Dumy, P (2007). Tumor targeting with RGD peptide ligands-design of new molecular conjugates for imaging and therapy of cancers. *Anticancer Agents Med Chem* **7**: 552-558.
11. Gestwicki, JE, Cairo, CW, Strong, LE, Oetjen, KA, and Kiessling, LL (2002). Influencing receptor-ligand binding mechanisms with multivalent ligand architecture. *J Am Chem Soc* **124**: 14922-14933.
12. Temming, K, Schifferers, RM, Molema, G, and Kok, RJ (2005). RGD-based strategies for selective delivery of therapeutics and imaging agents to the tumour vasculature. *Drug Resist Updat* **8**: 381-402.
13. Foillard, S, Jin, ZH, Garanger, E, Boturyn, D, Favrot, MC, Coll, JL, *et al.* (2008). Synthesis and biological characterisation of targeted pro-apoptotic peptide. *Chembiochem* **9**: 2326-2332.
14. Jin, ZH, Josserand, V, Razkin, J, Garanger, E, Boturyn, D, Favrot, MC, *et al.* (2006). Noninvasive optical imaging of ovarian metastases using Cy5-labeled RAFT-c(-RGDfK)-4. *Mol Imaging* **5**: 188-197.
15. Jin, ZH, Josserand, V, Foillard, S, Boturyn, D, Dumy, P, Favrot, MC, *et al.* (2007). In vivo optical imaging of integrin alphaV-beta3 in mice using multivalent or monovalent cRGD targeting vectors. *Mol Cancer* **6**: 41.
16. Sancey, L, Ardisson, V, Riou, LM, Ahmadi, M, Marti-Batlle, D, Boturyn, D, *et al.* (2007). In vivo imaging of tumor angiogenesis in mice with the alpha(v)beta (3) integrin-targeted tracer (99m)Tc-RAFT-RGD. *Eur J Nucl Med Mol Imaging* **34**: 2037-2047.
17. Garanger, E, Boturyn, D, Jin, Z, Dumy, P, Favrot, MC, and Coll, JL (2005). New multifunctional molecular conjugate vector for targeting, imaging, and therapy of tumors. *Mol Ther* **12**: 1168-1175.
18. Cheresch, DA, and Harper, JR (1987). Arg-Gly-Asp recognition by a cell adhesion receptor requires its 130-kDa alpha subunit. *J Biol Chem* **262**: 1434-1437.
19. Dedhar, S, Ruoslahti, E, and Pierschbacher, MD (1987). A cell surface receptor complex for collagen type I recognizes the Arg-Gly-Asp sequence. *J Cell Biol* **104**: 585-593.
20. Schifferers, RM, Ansari, A, Xu, J, Zhou, Q, Tang, Q, Storm, G, *et al.* (2004). Cancer siRNA therapy by tumor selective delivery with ligand-targeted sterically stabilized nanoparticle. *Nucleic Acids Res* **32**: e149.
21. Haubner, R, Weber, WA, Beer, AJ, Vabulienė, E, Reim, D, Sarbia, M, *et al.* (2005). Noninvasive visualization of the activated alphavbeta3 integrin in cancer patients by positron emission tomography and [18F]Galacto-RGD. *PLoS Med* **2**: e70.
22. Ellerby, HM, Arap, W, Ellerby, LM, Kain, R, Andrusiak, R, Rio, GD, *et al.* (1999). Anti-cancer activity of targeted pro-apoptotic peptides. *Nat Med* **5**: 1032-1038.
23. Castel, S, Pagan, R, Mitjans, F, Piulats, J, Goodman, S, Jonczyk, A, *et al.* (2001). RGD peptides and monoclonal antibodies, antagonists of alpha(v)-integrin, enter the cells by independent endocytic pathways. *Lab Invest* **81**: 1615-1626.
24. Schraa, AJ, Kok, RJ, Berendsen, AD, Moorlag, HE, Bos, EJ, Meijer, DK, *et al.* (2002). Endothelial cells internalize and degrade RGD-modified proteins developed for tumor vasculature targeting. *J Control Release* **83**: 241-251.
25. Pellinen, T, and Ivaska, J (2006). Integrin traffic. *J Cell Sci* **119**: 3723-3731.
26. Pizarro-Cerda, J, and Cossart, P (2006). Bacterial adhesion and entry into host cells. *Cell* **124**: 715-727.
27. Ramsay, AG, Marshall, JF, and Hart, IR (2007). Integrin trafficking and its role in cancer metastasis. *Cancer Metastasis Rev* **26**: 567-578.
28. Nemerow, GR, and Stewart, PL (1999). Role of alpha(v) integrins in adenovirus cell entry and gene delivery. *Microbiol Mol Biol Rev* **63**: 725-734.
29. Ning, Y, Buranda, T, and Hudson, LG (2007). Activated epidermal growth factor receptor induces integrin alpha2 internalization via caveolae/raft-dependent endocytic pathway. *J Biol Chem* **282**: 6380-6387.

30. De Deyne, PG, O'Neill, A, Resneck, WG, Dmytrenko, GM, Pumpllin, DW, and Bloch, RJ (1998). The vitronectin receptor associates with clathrin-coated membrane domains via the cytoplasmic domain of its beta5 subunit. *J Cell Sci* **111 (Pt 18)**: 2729-2740.
31. Alam, MR, Dixit, V, Kang, H, Li, ZB, Chen, X, Trejo, J, *et al.* (2008). Intracellular delivery of an anionic antisense oligonucleotide via receptor-mediated endocytosis. *Nucleic Acids Res* **36**: 2764-2776.
32. Wickham, TJ, Mathias, P, Cheresch, DA, and Nemerow, GR (1993). Integrins alpha v beta 3 and alpha v beta 5 promote adenovirus internalization but not virus attachment. *Cell* **73**: 309-319.
33. Adair, BD, Xiong, JP, Maddock, C, Goodman, SL, Arnaout, MA, and Yeager, M (2005). Three-dimensional EM structure of the ectodomain of integrin {alpha}V{beta}3 in a complex with fibronectin. *J Cell Biol* **168**: 1109-1118.
34. Boturyn, D, Coll, JL, Garanger, E, Favrot, MC, and Dumy, P (2004). Template assembled cyclopeptides as multimeric system for integrin targeting and endocytosis. *J Am Chem Soc* **126**: 5730-5739.
35. Dechantsreiter, MA, Planker, E, Matha, B, Lohof, E, Holzemann, G, Jonczyk, A, *et al.* (1999). N-Methylated cyclic RGD peptides as highly active and selective alpha(V)beta(3) integrin antagonists. *J Med Chem* **42**: 3033-3040.
36. Heckmann, D, Meyer, A, Marinelli, L, Zahn, G, Stragies, R, and Kessler, H (2007). Probing integrin selectivity: rational design of highly active and selective ligands for the alpha5beta1 and alphavbeta3 integrin receptor. *Angew Chem Int Ed Engl* **46**: 3571-3574.
37. Kato, M, and Mrksich, M (2004). Using model substrates to study the dependence of focal adhesion formation on the affinity of integrin-ligand complexes. *Biochemistry* **43**: 2699-2707.
38. Kumar, CC, Nie, H, Rogers, CP, Malkowski, M, Maxwell, E, Catino, JJ, *et al.* (1997). Biochemical characterization of the binding of echistatin to integrin alphavbeta3 receptor. *J Pharmacol Exp Ther* **283**: 843-853.
39. Pfaff, M, Tangemann, K, Muller, B, Gurrath, M, Muller, G, Kessler, H, *et al.* (1994). Selective recognition of cyclic RGD peptides of NMR defined conformation by alpha IIb beta 3, alpha V beta 3, and alpha 5 beta 1 integrins. *J Biol Chem* **269**: 20233-20238.
40. Takagi, J, Petre, BM, Walz, T, and Springer, TA (2002). Global conformational rearrangements in integrin extracellular domains in outside-in and inside-out signaling. *Cell* **110**: 599-511.
41. Dormond, O, Ponsonnet, L, Hasmim, M, Foletti, A, and Rugg, C (2004). Manganese-induced integrin affinity maturation promotes recruitment of alpha V beta 3 integrin to focal adhesions in endothelial cells: evidence for a role of phosphatidylinositol 3-kinase and Src. *Thromb Haemost* **92**: 151-161.
42. Legler, DF, Wiedle, G, Ross, FP, and Imhof, BA (2001). Superactivation of integrin alphavbeta3 by low antagonist concentrations. *J Cell Sci* **114**: 1545-1553.
43. Verdaguer, N, Schoehn, G, Ochoa, WF, Fita, I, Brookes, S, King, A, *et al.* (1999). Flexibility of the major antigenic loop of foot-and-mouth disease virus bound to a Fab fragment of a neutralising antibody: structure and neutralisation. *Virology* **255**: 260-268.
44. Fender, P, Schoehn, G, Perron-Sierra, F, Tucker, GC, and Lortat-Jacob, H (2008). Adenovirus dodecahedron cell attachment and entry are mediated by heparan sulfate and integrins and vary along the cell cycle. *Virology* **371**: 155-164.
45. Bartlett, JS, Wilcher, R, and Samulski, RJ (2000). Infectious entry pathway of adeno-associated virus and adeno-associated virus vectors. *J Virol* **74**: 2777-2785.
46. Memmo, LM, and McKeown-Longo, P (1998). The alphavbeta5 integrin functions as an endocytic receptor for vitronectin. *J Cell Sci* **111 (Pt 4)**: 425-433.
47. del Pozo, MA, Balasubramanian, N, Alderson, NB, Kiosses, WB, Grande-Garcia, A, Anderson, RG, *et al.* (2005). Phospho-caveolin-1 mediates integrin-regulated membrane domain internalization. *Nat Cell Biol* **7**: 901-908.
48. Soumpasis, DM (1983). Theoretical analysis of fluorescence photobleaching recovery experiments. *Biophys J* **41**: 95-97.
49. Klein, C, Pillot, T, Chambaz, J, and Drouet, B (2003). Determination of plasma membrane fluidity with a fluorescent analogue of sphingomyelin by FRAP measurement using a standard confocal microscope. *Brain Res Brain Res Protoc* **11**: 46-51.
50. Roberts, M, Barry, S, Woods, A, van der Sluijs, P, and Norman, J (2001). PDGF-regulated rab4-dependent recycling of alphavbeta3 integrin from early endosomes is necessary for cell adhesion and spreading. *Curr Biol* **11**: 1392-1402.

Table 1: Integrin $\alpha_v\beta_3$ internalization assay.

Peptide	Concentrations (μM)	% Internalized integrins	Variation (%) ^(a)
	none	11.99 \pm 1.13	-
RAFT-RGD	0.1	17.18 \pm 1.08	+ 43% *
	0.5	20.05 \pm 2.08	+ 67% **
	1	21.41 \pm 1.85	+ 79% ***
	1 + Amantadine	12.03 \pm 1.58	+ 0% ** (b)
	1 + Nystatin	19.67 \pm 1.42	+ 64% ^{NS} (b)
	1 + Amiloride	19.91 \pm 2.80	+ 66% ^{NS} (b)
cRGD	0.1	11.67 \pm 1.31	- 3% ^{NS}
	0.5	10.76 \pm 1.08	- 10% ^{NS}
	1	11.77 \pm 1.00	- 2% ^{NS}
	4	9.24 \pm 1.23	- 23% ^{NS}

* $P < 0.05$, ** $P < 0.01$, *** $P < 0.001$ vs. control

(a) Variations of internalization were compared to the control condition (absence of peptide). Results were expressed as mean \pm S.E.M. and each experiment was performed in quadruplet at least.

(b) P values calculated vs. RAFT-RGD 1 μM .

Figure legends

Figure 1: RGD-peptides affinities.

(a) Chemical structures of RGD peptides. The monovalent *cyclo*[-RGDfK-] (cRGD) was compared with the tetrameric RAFT(c[-RGDfK-]₄) (RAFT-RGD). cRGD was modified on the lysine side chain to obtain the fluorochrome-conjugated cRGD-FITC or cRGD-Cy5. For RAFT-RGD, fluorochromes were conjugated to the lower face of the RAFT scaffold (central alanine residues replaced by lysine). RAFT(c[-R β ADfK-]₄) (RAFT-RAD) was used as negative control.

(b) FCS analysis of the interaction of Cy5-labeled peptides with soluble integrins at 633 nm. K_D was determined at the equilibrium. The diffusion time τ_D and the diffusion coefficients D of the peptides alone or in a complex with the integrin are indicated. Data were best-fitted by a two-components model and are represented as mean \pm standard deviation (SD). Representative plots are available in the supplementary data file.

Figure 2: RAFT-RGD-FITC reduces $\alpha_v\beta_3$ integrin lateral mobility.

R-PhycoErythrin-conjugated LM609 monoclonal antibody was used for direct observation of $\alpha_v\beta_3$ integrin diffusion on the apical membrane of the cell. Adherent HEK293(β_3) cells were incubated with 0.5 μ M FITC-labeled RAFT-RGD or RAFT-RAD or 2 μ M cRGD-FITC or in absence of peptides. The antibody LM609-RPE was also present during the 8 min of incubation with the peptides in order to follow integrin lateral diffusion. After washing, the cells were observed on an inverted confocal microscope. Recovery of the integrin signal into the bleached area is significantly slowed down in the condition where cells were incubated in the presence of the multimeric RGD-presenting ligand, RAFT-RGD-FITC, as compared to non-treated cells, or

to RAFT-RAD-FITC or cRGD-FITC treated cells.

Figure 3: RGD-peptides/integrin $\alpha_v\beta_3$ complexes.

Representative examples of negatively stained electron micrographs of the soluble $\alpha_v\beta_3$ integrin alone or mixed with RGD-peptides. The $\alpha_v\beta_3$ integrins remain in monomeric state except when using RAFT-RGD; in this condition, integrins can be found as dimers on the grid. As expected, RGD-peptides (<6 kDa) were not distinguishable. Upper panels: Original images. Lower panels: Photoshop enhanced visualization of the complexes.

Figure 4: Confocal imaging on HEK293(β_3) living cells.

Cells were starved for 30 min and incubated with 1 mM RAFT-RGD-Cy5 (a - d) or 1 mM cRGD-Cy5 (e - h) for 10 min at room temperature in DMEM medium alone (a, e) or containing amantadine 1 mM (b, f), nystatin 1 μ M (c, g) or amiloride (d, h). Cells were then rinsed and observed at 633 nm. Peptide internalization was evaluated according to the Cy-5 intensity in the cells and is indicated for each photo. Scale bar: 10 μ m.

Table 1: Integrin $\alpha_v\beta_3$ internalization assay. HEK293(β_3) membrane proteins were biotinylated and the cells were incubated in presence of 0 to 1 μM RAFT-RGD or 0 to 4 μM cRGD for 10 min. The cells were then lysed and the concentration of biotinylated- $\alpha_v\beta_3$ -integrins present into each fraction measured using ELISA. Variations of internalization were compared to the control condition (absence of peptide).

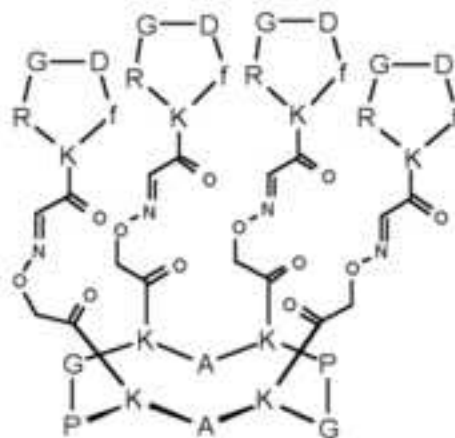
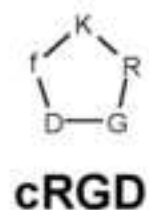
Peptide	Concentrations (μM)	% Internalized integrins	Variation (%)
RAFT-RGD	none	11.99 ± 1.13	-
	0.1	17.18 ± 1.08	+ 43% *
	0.5	20.05 ± 2.08	+ 67% **
	1	21.41 ± 1.85	+ 79% ***
	1 + Amantadine	12.03 ± 1.58	+ 0% ** (1)
	1 + Nystatin	19.67 ± 1.42	+ 64% ^{NS} (1)
	1 + Amiloride	19.91 ± 2.8	+ 66% ^{NS} (1)
	cRGD	0.1	11.67 ± 1.31
0.5		10.76 ± 1.08	- 10% ^{NS}
1		11.77 ± 1.00	- 2% ^{NS}
4		9.24 ± 1.23	- 23% ^{NS}

* $P < 0.05$, ** $P < 0.01$, *** $P < 0.001$ vs. control;

(1) P values calculated vs. RAFT-RGD 1 μM .

Figure-1
[Click here to download high resolution image](#)

a



b

Molecule	MW (g.mol ⁻¹)	Soluble integrin	τ_D (μ s)	D_{peptide} ($\times 10^{10} \text{ m}^2 \cdot \text{s}^{-1}$)	D_{complex} ($\times 10^{11} \text{ m}^2 \cdot \text{s}^{-1}$)	$K_D \pm \text{SD}$ (nM)
RAFT-(cRGD) ₄	4517.12	$\alpha_v\beta_3$	-	-	-	-
RAFT-(cRGD) ₄ -Cy5	4556.16	$\alpha_v\beta_3$	112	1.72	1.89	3.87 \pm 1.42
cRGD-Cy5	1280.59	$\alpha_v\beta_3$	77	2.72	2.64	41.70 \pm 17.13
RAFT-(cRAD) ₄ -Cy5	4612.27	$\alpha_v\beta_3$	106	1.69	-	> 10000
RAFT-(cRGD) ₄ -Cy5	4556.16	$\alpha_3\beta_1$	112	1.72	4.72	1147.58 \pm 174.71

Figure-2
[Click here to download high resolution image](#)

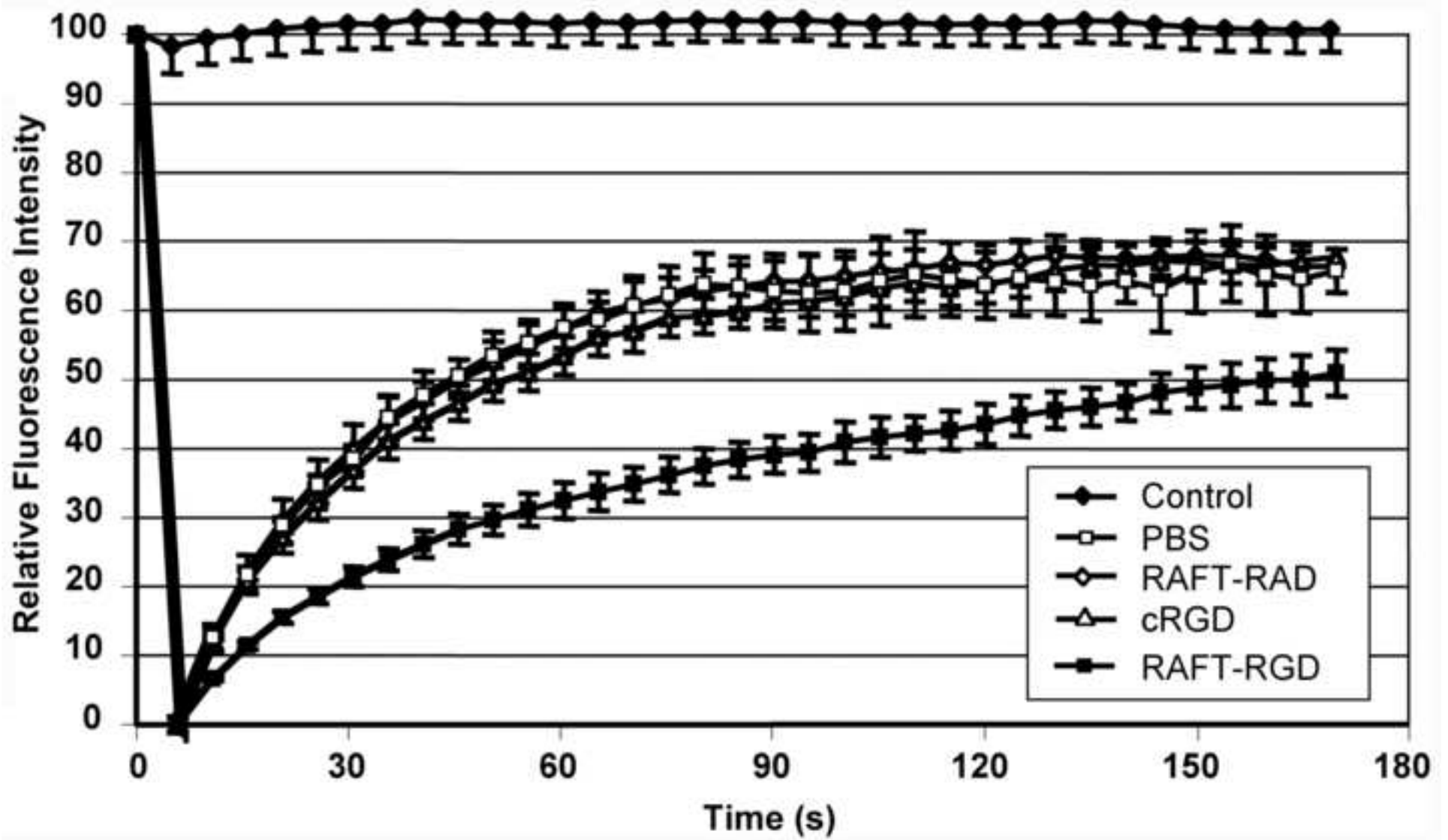


Figure-3

[Click here to download high resolution image](#)

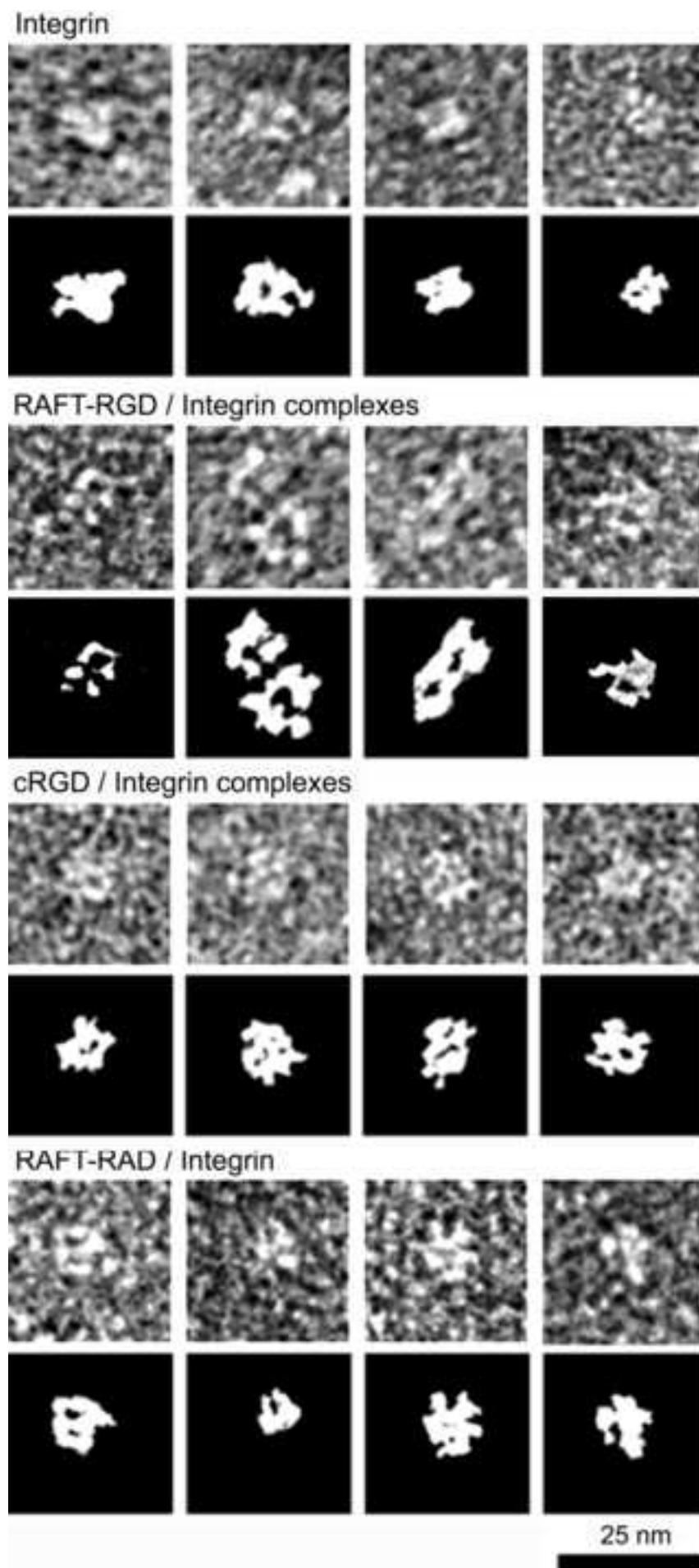
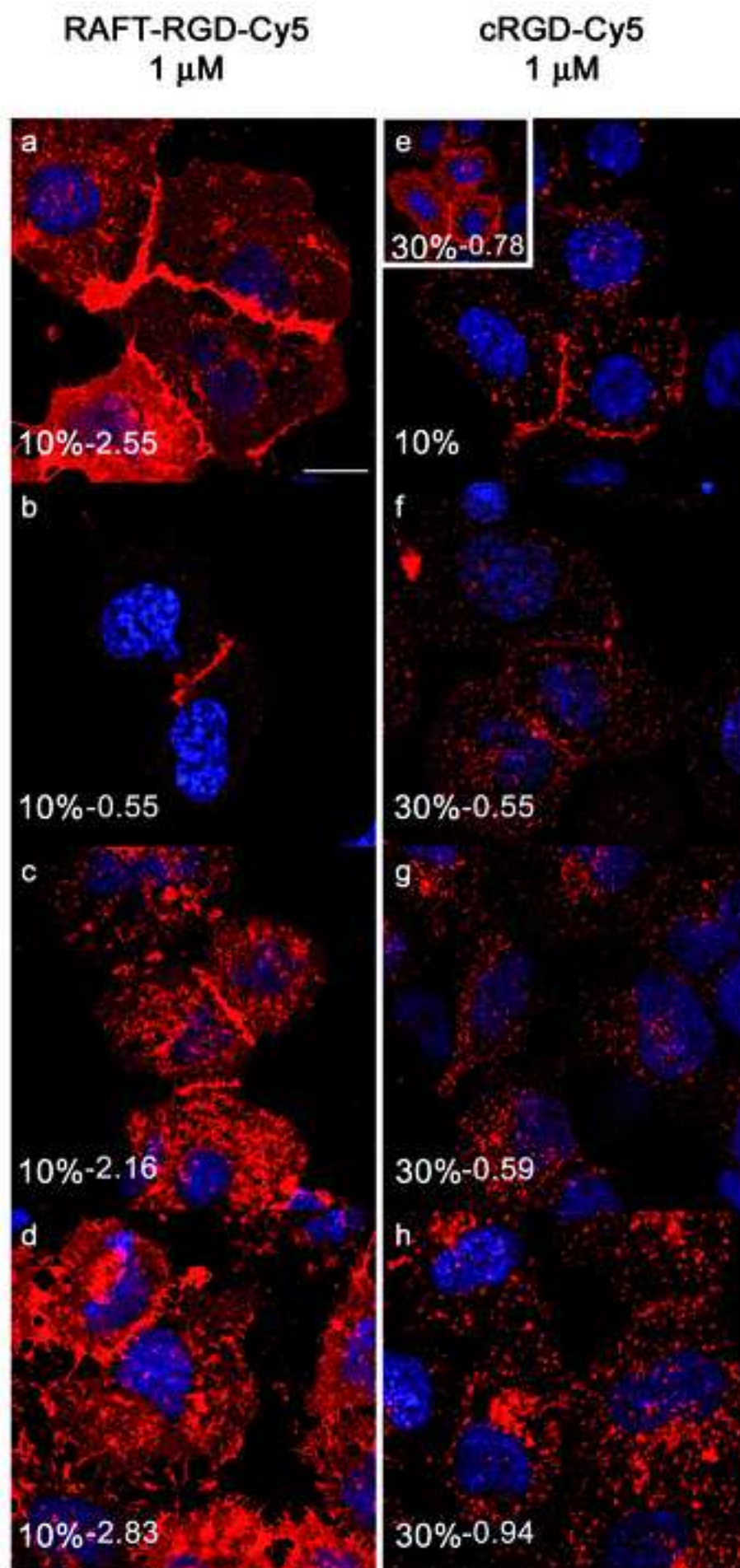
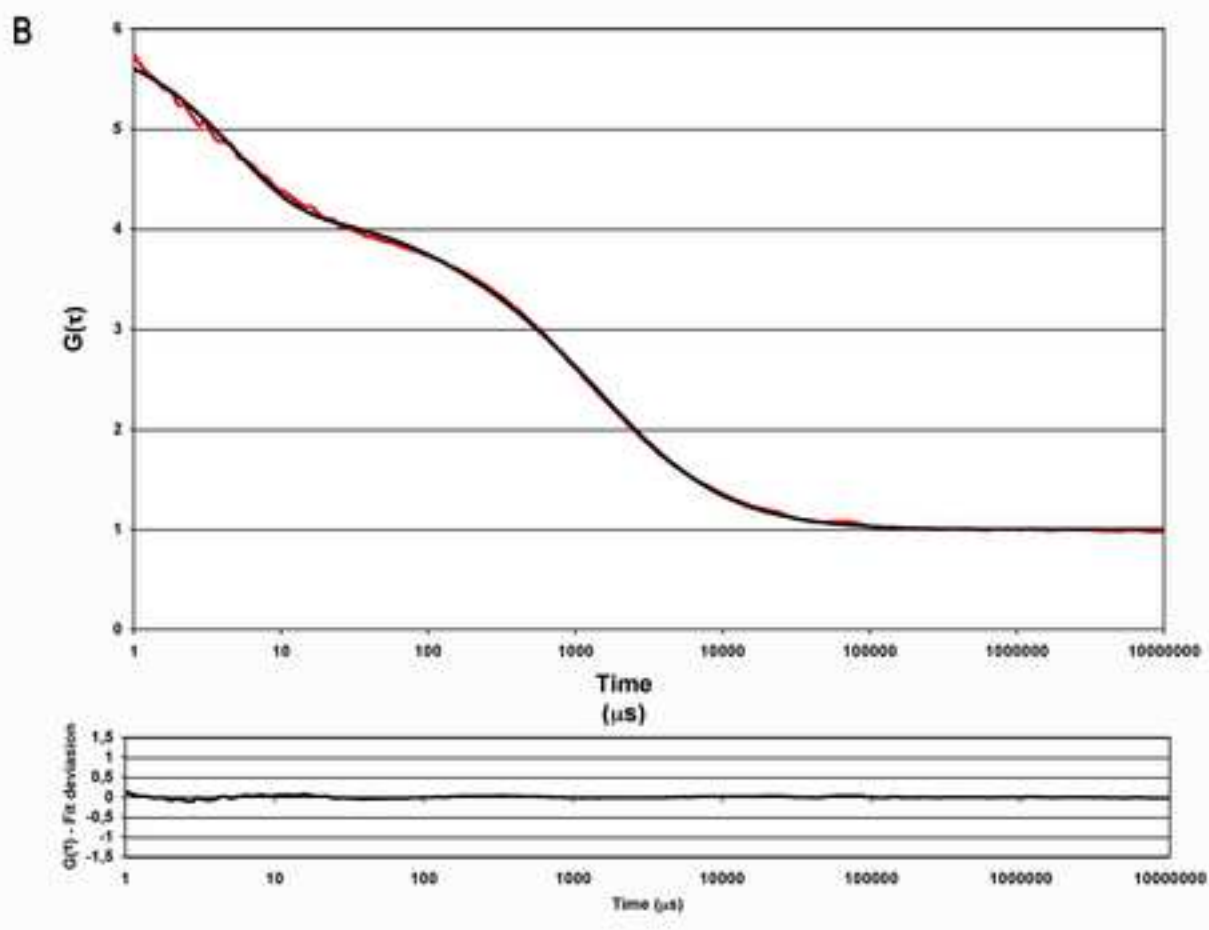
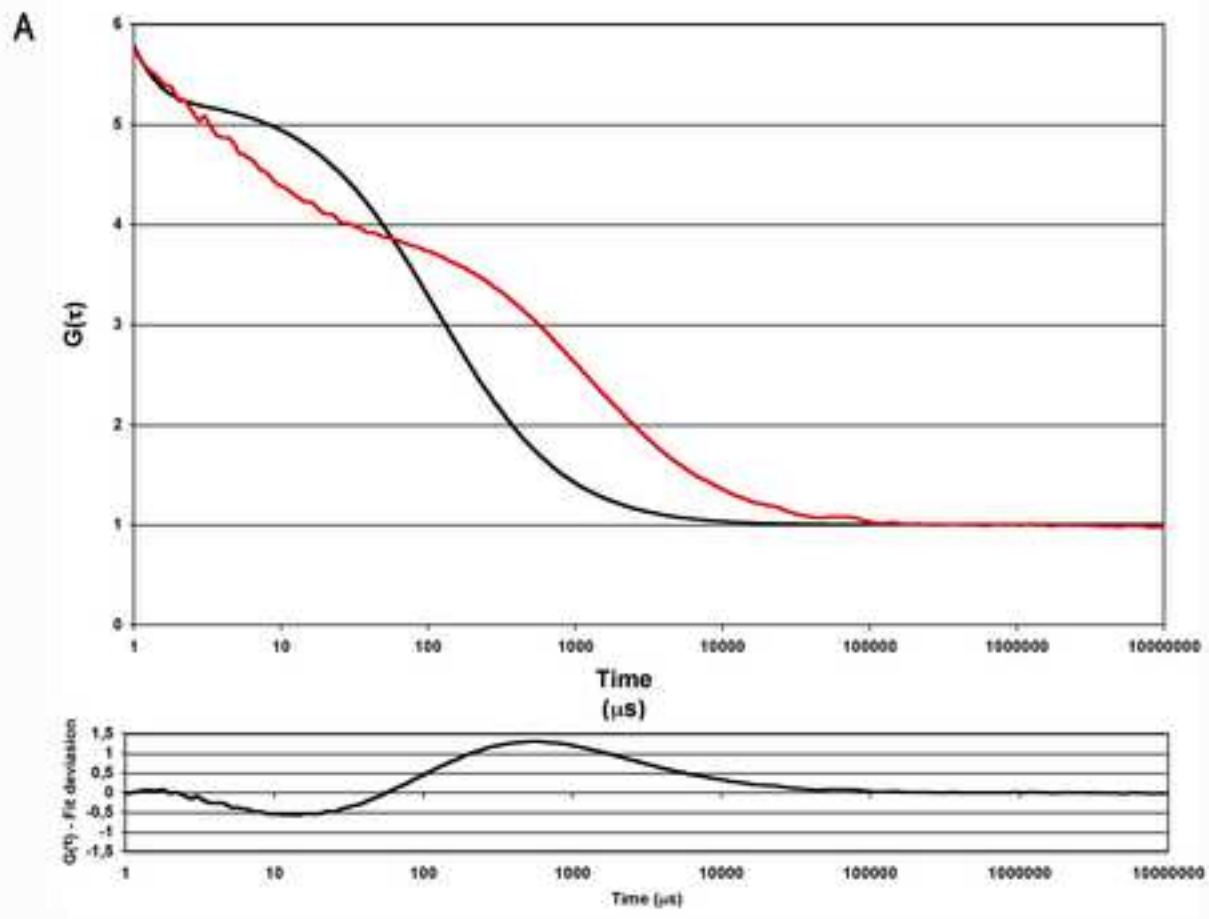


Figure-4

[Click here to download high resolution image](#)





Supplementary data

Fig.1Sup: Curve fitting of FCS analysis. Curve fitting of RAFT-RGD-Cy5 mixed with integrin $\alpha_v\beta_3$ and the corresponding residuals curves using a one-compartment (A) and a two-compartment model (B). χ^2 values are $5.3E^{-2}$ and $1.9E^{-4}$, respectively. Using the three-compartment model, the same kinds of curves as in (B) was found, with two similar diffusion times of the complex RAFT-RGD-Cy5/integrin ($\pm 3 \mu\text{s}$).